Cite this article
Sankar AS, Hari R and Mini KM
Effect of micro silica and aggregate size on cracking of self-compacting concrete.
Proceedings of the Institution of Civil Engineers – Construction Materials,
https://doi.org/10.1680/jcoma.18.00080

Research Article
Paper 1800080
Received 13/10/2018;
Accepted 22/01/2019

Keywords: concrete technology & manufacture/mathematical modelling/ strength & testing of materials

Construction Materials

ICE Publishing

Effect of micro silica and aggregate size on cracking of self-compacting concrete

Aswathy S. Sankar MTech
Postgraduate student, Department of Civil Engineering, Amrita School of Engineering, Amrita Vishwa Vidyapeetham, Coimbatore, India

Rahesh Hari MTech
Postgraduate student, Department of Civil Engineering, Amrita School of Engineering, Amrita Vishwa Vidyapeetham, Coimbatore, India

K. M. Mini PhD
Professor and Chairperson, Department of Civil Engineering, Amrita School of Engineering, Amrita Vishwa Vidyapeetham, Coimbatore, India
(corresponding author: k_mini@cb.amrita.edu)
(Orcid:0000-0002-5601-2209)

In the evaluation of long-term serviceability leading to prevention of damage of self-compacting concrete (SCC) structures, a thorough understanding on fracture parameters and cracking performance from initial stage to hardened stage is important. This paper reports the effect of coarse aggregate size and micro silica addition on fracture characteristics and ductility of SCC. Experiments were performed by conducting three-point bending tests on notched beams as per recommendations by Rilem standards. For all mixes, the parameters are analysed by the size-effect method. The tests proved that an increase in the size of the coarse aggregates can increase the fracture energy and ductility due to changing fractal dimensions and the fracture process zone length. A 10% addition of micro silica showed better fracture properties. Equations for assessing the fracture energy and length of the fracture process zone using a statistical approach were then developed.

Notation

A	angular coefficient
a_0	notch depth
B, d_0	empirical coefficients
b	beam width
C	Y-intercept of the regression line
C_f	length of fracture process zone
C_n	convenience coefficient
d	beam depth
d_{max}	maximum aggregate size
E	elasticity modulus
G_f	fracture energy
$g(\alpha_0)$	non-dimensional rate of energy release
$g'(\alpha_0)$	derivative of $g(\alpha_0)$ with respect to the initial crack length ($\alpha_0 = a_0/d$)
K_{IC}	fracture toughness
P_u	peak load
β	brittleness number
δ_c	displacement at peak loads
σ_N	normal strength of member

1. Introduction

The presence of dense reinforcement in structures makes concreting tedious, resulting in highly non-homogeneous reinforced concrete with voids/honeycombs. Mechanical or manual compaction methods are difficult to perform in such conditions, which adds to the total expense and duration of the project. The use of self-compacting concrete (SCC) is promising under such conditions as it does not require any vibrations. The flowability is high compared with normal concrete and hence this concrete can fill the corners of the form without any external compacting effort. To enhance flowability and passing ability through narrowly spaced reinforcement, SCC has limitations on the maximum size, amount and gradation of aggregates. In spite of being a highly workable mix, the chances of segregation and the loss of entrained air voids are greater in SCC. These issues can be eliminated by lower water–cement ratio, higher fine-to-coarse aggregate ratio, high-range water-reducing admixtures and better aggregate gradation.

Although SCC is highly advantageous, it consumes a large amount of mineral particles, finer coarse aggregates and superplasticisers (SPs). Differences in the mixing of these components results in variation in mechanical and fracture characteristics with varied cracking patterns. Glucklich (1963) observed that the energy for crack propagation in cement paste is more owing to the formation of micro cracks near the crack tip due to its non-ductile behaviour. The properties of cracking concrete can be appropriately represented by the concept of non-linear fracture mechanics, which considers the fracture process zone. Bazant and Oh (1983) divided the fracture process zone models into two categories, namely, the fictitious crack approach and the effective crack approach based on the differences in energy dissipation mechanisms.

Jenq and Shah (1985) reported that many of the crack models require two factors, crack tip opening displacement and critical stress intensity factor, for defining the elastic fracture process and to monitor crack propagation. These two parameters are proved to be independent of the size but dependent on the type of material. The first to propose the fictitious crack model was Hillerborg *et al*. (1976). Beygi *et al*. (2014a) showed that the fracture energy and the length of the fracture process zone increased with an increase in the size and volume of coarse aggregates in SCC mixes. The effect of powder additive on the fracture characteristics of SCC was examined by Nikbin *et al*. (2014), who proved that fracture energy and length of fracture process zone increased with increase in the mineral filler content. Craeye *et al*. (2010) observed that limestone powder as a mineral additive in SCC mixes can have more endogenous shrinkage and hence higher cracking probability. Yang *et al*. (2009) proved that the usage of ultra-fine particles like limestone powder improved the compactness of the SCC matrix and reduced the porosity of the interfacial transition zone (ITZ) of aggregates and pastes. In normal concrete, Kwon *et al*. (2008) observed that a decrease in ITZ strength leads to a significant increase in fracture energy. Beygi *et al*. (2014b) reported that the properties of ITZ become more critical by increasing the maximum size of aggregates (d_{max}). The impact of the maximum size of aggregates on fracture energy in normally vibrated concrete was analysed by Hillerborg *et al*. (1976) and they observed that fracture energy tends to increase when d_{max} increases from 8 to 20 mm. Trunk and Wittmann (1998) and Ghaemmaghami and Ghaemian (2006) observed that in dam concrete the highest value for fracture energy is obtained with the highest d_{max}. They generated a power function between d_{max} and fracture energy. Mrudul *et al*. (2017) performed a design of experiments by considering silica percentage and recycled aggregate percentage replacement as the factors and the flowability and compressive strength as responses and obtained relations connecting them.

This paper reports an experimental programme on the effect of micro silica and the size of coarse aggregates on the fracture properties and ductility of SCC mixes. Fracture parameters are evaluated using the size-effect method (SEM) because the effect of structural size is important as geometrically similar specimens show a pronounced size effect on their failure load. Therefore, it is important to establish a relationship between the size-effect behaviour and the fracture properties of concrete. The tests are performed using a servo displacement controlled testing system of capacity 150 kN on different sizes of notched beams subjected to three-point bending as per Rilem FMT-89 (Rilem TCS, 1990) and Rilem FMC-50 (Rilem TCS, 1985). Relations are also developed between the various fracture parameters using a statistical approach (Box *et al*., 2005).

2. Fracture parameters evaluation

In SEM, fracture parameters are identified with the help of three-point bending tests on notched beams of similar geometry and varied sizes. Normal strength as explained by the size-effect law of geometrically similar concrete beams can be represented as

1. $$\sigma_N = \frac{B}{\sqrt{(1+\beta)}}$$

2. $$\beta = \frac{d}{d_0}$$

where β is the brittleness number (Bazant and Planas, 1997), and B and d_0 are empirical coefficients in connection with structural geometry and material properties. σ_N is the normal strength of a member which has similar dimensions in two directions is given by

3. $$\sigma_N = \frac{C_n P_u}{bd}$$

where P_u is the peak load obtained, C_n is the convenience coefficient, d is the beam depth and b is the beam width.

On the basis of Equations 1–3, when $\beta < 0{\cdot}1$ the behaviour of the structure approaches ductile and starts to follow a strength criterion, whereas when $\beta > 10$ it follows linear elastic fracture mechanics (LEFM) as it becomes brittle and, for $0{\cdot}1 \leq \beta \leq 10$, it follows non-linear elastic fracture mechanics (NLFM) behaviour. Thus, it can be observed that with an increase in the depth of geometrically similar specimens, the failure mode gradually changes from ductile to brittle. Therefore, it is reasoned that if the maximum loads of geometrically similar specimens with varying sizes are extrapolated to specimens of infinite sizes, the acquired fracture energy is unique and as a result will be independent of the size of the specimen; therefore, LEFM assumptions can be adopted. Thus, the coefficients B and d_0 can be obtained with the help of a linear regression of the maximum loads of beams of similar geometry of different sizes, as per Rilem FMT-89 (Rilem TCS, 1990)

4. $$Y = AX + C$$

where

5. $$Y = \left(\frac{1}{bd}\right)^2, \; X = d, \; B = \frac{1}{\sqrt{C}}, \; d_0 = \frac{C}{A}$$

Hence it can be concluded that in the failure of the structures of infinite sizes, the two important properties, length of fracture process zone (C_f) and fracture energy (G_f) can be determined using

6. $$G_F = \frac{g(\alpha_0)}{AE}$$

7. $$C_F = \frac{g(\alpha_0)}{g'(\alpha_0)} \times \left(\frac{C}{A}\right)$$

where C is the Y-intercept of the regression line, A is an angular coefficient of the regression line obtained, E is the elasticity modulus of the concrete, $g(\alpha_0)$ is a non-dimensional rate of energy release and $g'(\alpha_0)$ is the derivative of $g(\alpha_0)$ with respect to the initial crack length ($\alpha_0 = a_0/d$). $g(\alpha_0)$ and $g'(\alpha_0)$ functions are geometrically dependent and can be acquired using LEFM concepts. $g(\alpha)$ can be obtained from Rilem-TC 89 (Rilem TCS, 1990). Using SEM, the other parameters such as the effective crack tip opening, displacement at peak loads (δ_c) and fracture toughness (K_{IC}) can also be obtained (Rilem FMT-89 (Rilem TCS, 1990)).

Table 1. Properties of materials

Cement (Portland pozzolana cement)	
Fineness	1%
Specific gravity	2·97
Normal consistency	34%
Fine aggregate	
Specific gravity	2·66
Bulk density	1·67 kg/l
Fineness	3·718
Coarse aggregate	
Specific gravity	2·45
Water absorption	0·250
Bulk density	1·63 kg/l
Micro silica	
Specific gravity	2·5

Table 2. SCC mix designations

Aggregate size range: mm	Micro silica addition level: %	Mix designation
12·5–10	5	SC1
	10	SC2
	15	SC3
10–6	5	SC4
	10	SC5
	15	SC6
6–4·75	5	SC7
	10	SC8
	15	SC9

3. Experimental investigation

3.1 Materials

Portland pozzolana cement of brand ACC is used to prepare the concrete. Micro silica with a specific gravity of 2·66 is used to study the effect. Poly-carboxylate ether (PCE)-based SP is used. River sand with a fineness modulus of 3·71 is used as fine aggregates. Naturally crushed gravels with maximum sizes of 6, 10 and 12·5 mm and acquired from a single source are used as coarse aggregates. The properties of the materials used are listed in Table 1.

3.2 Mix design

In total, nine mixes are considered to evaluate the influence of the size of coarse aggregates and micro silica on the fracture properties of SCC. Three different coarse aggregates with sizes in the ranges of 12·5–10, 10–6 and 6–4·75 mm with varying addition levels of micro silica at 5, 10 and 15% are used. The mix designations and proportions of the nine mixes are presented in Tables 2 and 3. The fresh stage properties of SCC mixes are examined by conducting L-box, slump flow and sieve segregation tests as per EFNARC recommendations (EFNARC, 2002) and are presented in Table 3. SP dosage is varied to obtain adequate flow with different coarse aggregate sizes.

3.3 Specimen preparations and testing procedures

Six standard cylinders 150 mm × 300 mm and three standard cubes 150 mm × 150 mm × 150 mm are made in addition to the bending test specimens from each mix. The specimens are water cured for 28 d. The compressive strength f_c, modulus of elasticity E and splitting tensile strength f_t are obtained after 28 d of curing (Table 4).

Three-point bending experiments are performed to obtain the relationships between micro silica, size of coarse aggregates

Table 3. Compositions and fresh stage properties of SCC mixes

Materials	SC1	SC2	SC3	SC4	SC5	SC6	SC7	SC8	SC9
Cement: kg/m^3	540	540	540	540	540	540	540	540	540
Fine aggregate: kg/m^3	827·8	827·8	827·8	827·8	827·8	827·8	827·8	827·8	827·8
Coarse aggregate: kg/m^3	817	817	817	817	817	817	817	817	817
Water/cement (W/C)	0·38	0·38	0·38	0·38	0·38	0·38	0·38	0·38	0·38
SP: %	1	1	0·9	0·9	0·85	0·9	0·9	0·9	0·9
Micro silica: %	5	10	15	5	10	15	5	10	15
Slump flow: mm	710	705	730	735	728	740	690	715	720
T_{50} slump flow: s	2·1	2	2	1·7	1·8	2	2·5	2·2	2·7
L-box (H_2/H_1)	0·81	0·8	0·86	0·82	0·91	0·86	0·84	0·83	0·92
V funnel: s	12	11·4	12	10	10·2	12	8	8·1	8
T_5 V funnel: s	15	15	15·3	14·5	15	15	11	11·3	12
J ring: mm	8	6	5	5	7	8	6	7	6

Table 4. Strength properties of the mixes

Parameters	SC1	SC2	SC3	SC4	SC5	SC6	SC7	SC8	SC9
Compressive strength: N/mm^2	55·55	72	67·11	55·11	71·11	64	54·22	63·11	54·67
Tensile strength: N/mm^2	5·09	5·41	5·09	4·29	5·41	4·29	3·97	5·09	5·09
Modulus of elasticity: GPa	33·6	34·5	33·18	33·2	33·7	32·6	33·9	34·68	32·4

and the fracture parameters of the SCC mixes. Notched beams as shown in Figures 1 and 2 are subjected to a constant displacement loading condition. The width of the beam, proportions of the span to depth, and length to depth are maintained constant. Samples of different sizes with geometrical similarity in two adjacent dimensions and constant width are used to examine the fracture parameters. By considering the maximum aggregate size and Rilem TC 89 recommendations (Rilem TCS, 1990), the ratio of the depth of notches to the depth of beams in all the specimens is adopted as 0·2 ($a_0 = 0{\cdot}2d$) and the tests are conducted in displacement-controlled mode. The specimens are loaded in a 150 kN capacity universal testing machine having closed-loop electro servo displacement-controlled system (Figure 3). The loads are applied at a constant rate of displacement such that the peak loads of all the specimens are achieved at a constant rate of 0·1 mm/min. Table 5 represents the dimensions of the beam specimen (Figures 1 and 2).

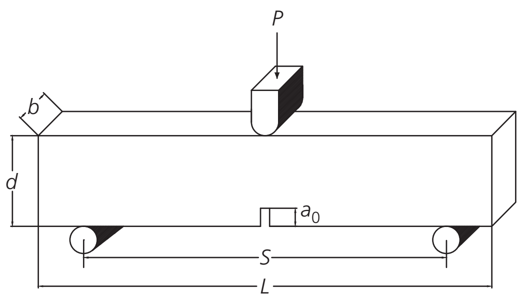

Figure 1. Notched beam basic geometry

4. Results and discussion

As per Rilem-TC 89 (Rilem TCS, 1990), estimation of the fracture parameters involves corrected peak load values that are obtained by adding half of the beam mass to the peak load. Table 6 reports the corrected peak loads for all geometrically similar specimens with varying sizes. Linear regression analysis of each mix is carried out using corrected peak load values and Equations 1–5 (Figure 4). Two important fracture parameters, namely, the effective length of process zone (C_f) and initial fracture energy (G_f), are tabulated using Equations 6 and 7 and the results are presented in Table 7. The fracture energy is observed to increase with an increase in d_{max}. The same trend was reported by Jenq and Shah (1985)

Figure 2. Notched beam

Figure 3. Test set-up

Table 5. Dimensions of notched beam specimens

Aggregate size range: mm	Depth, d: mm	Breadth, b: mm	Length, l: mm	Notch depth, a_0	l/d	a_0/d
6–4·75	24	24	64·08	4·8	2·67	0·2
	48	24	128·16	9·6	2·67	0·2
	96	24	256·32	19·2	2·67	0·2
10–6	40	40	106·8	8	2·67	0·2
	80	40	213·6	16	2·67	0·2
12·5–10	50	50	133·5	10	2·67	0·2
	100	50	267	20	2·67	0·2

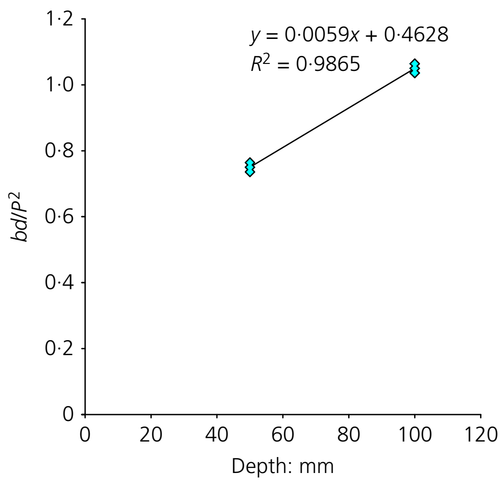

Figure 4. Linear regression of SC1 mix

Table 6. Corrected maximum loads for mixes

Mix	Depth: mm	Corrected peak loads: N		
		Beam 1	Beam 2	Beam 3
SC1	50	2398	2182	2312
	100	4014	4102	4051
SC2	50	2857	2924	2832
	100	4871	4830	4907
SC3	50	2694	2658	2576
	100	4331	4387	4380
SC4	40	1922	1901	1798
	80	3133	3096	3121
SC5	40	2076	2212	2235
	80	3464	3444	3483
SC6	40	1897	1962	1915
	80	3139	3163	3181
SC7	24	1196	1124	1117
	48	2142	2308	2284
	96	2767	2781	2755
SC8	24	1688	1393	1672
	48	2186	2175	2218
	96	3167	3153	3085
SC9	24	1198	1173	1129
	48	1582	1564	1553
	96	2377	2421	2391

where G_f varied from 21·1 to 35·4 N/m with an increase in d_{max} from 4·75 to 19 mm. Beygi *et al.* (2014a) reported that the strength of ITZ reduces with an increase in the value of d_{max}. Thereby, large-sized aggregates get pulled out rather than fracture, which leads to an increase in the roughness on the surface of fracture and consumption of more energy (Beygi *et al.*, 2014a). Less brittleness is observed due to the higher value of C_f in the SCC mixes. An improvement in ductility of concrete with an increase in d_{max} has been reported by Moseley *et al.* (1987). An increase in the value of the fracture parameter C_f decreases the brittleness of concrete. As per Bazant and Oh (1983), the value of C_f in normally vibrated concrete varies from 10 to 25 mm. In this study, with an increase in the size of aggregate from 6 to 12·5 mm, C_f increases. This shows that concrete ductility tends to increase with an increase in d_{max}. This is due to the reduction in strength and change in the microstructure of ITZ with an increase in d_{max}. The debonding of the coarse aggregates used and the lengthening of the path of fracture tend to increase the fracture dimensions (Beygi *et al.*, 2014a; Nikbin *et al.*, 2014). Failure loads in concrete structures can be predicted with the help of G_F and C_F).

A statistical approach using design of experiments is carried out to arrive at relations between various fracture parameters and the variables. Using the results obtained for SCC mixes with varied aggregate sizes and micro silica addition levels, equations are developed for the total fracture energy with respect to aggregate size and micro silica addition level.

$$\begin{aligned}\text{Fracture energy} = & -72{\cdot}7138 + 48{\cdot}87805 \times \text{ms} \\ & + 19{\cdot}25449 \times d_{max} \\ & - 9{\cdot}98617 \times \text{ms} \times d_{max} \\ & - 2{\cdot}87415 \times \text{ms}^2 \\ & - 1{\cdot}01872 \times d_{max}^2 \\ & + 0{\cdot}59112 \times \text{ms}^2 \times d_{max} \\ & + 0{\cdot}53466 \times \text{ms} \times d_{max}^2\end{aligned} \quad (8)$$

where d_{max} is the maximum aggregate size and ms is the micro silica addition level.

Table 7. Fracture parameters of the mixes

Parameters	SC1	SC2	SC3	SC4	SC5	SC6	SC7	SC8	SC9
a_0/d	0·2	0·2	0·2	0·2	0·2	0·2	0·2	0·2	0·2
$g(\alpha_0)$	7·268	7·268	7·268	7·268	7·268	7·268	7·268	7·268	7·268
G_f: N/m	36	42·13	27·38	27·36	30·8	27·86	35·73	41·91	24·92
C_f: mm	69·86	45·09	29·28	24·827	16·17	21·83	3·17	0·29	2·819
K_{IC}: MPamm$^{0·5}$	34·77	38·12	30·14	30·13	32·217	30·13	34·80	38·12	28·41

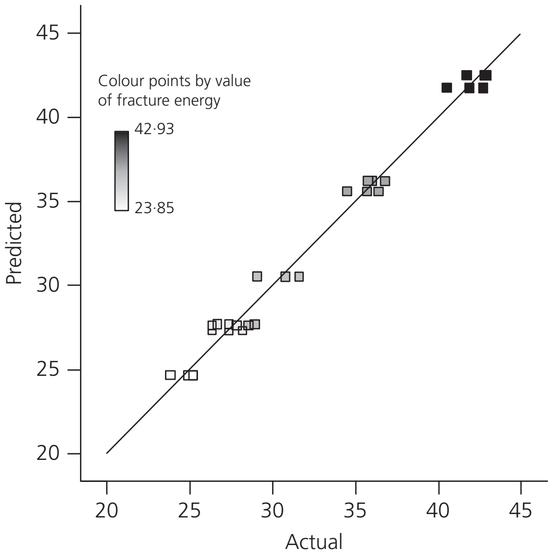

Figure 5. Predicted against actual fracture energy

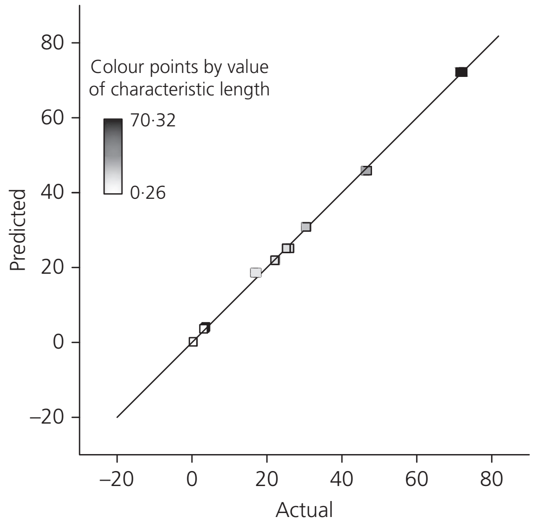

Figure 6. Predicted against actual length of the fracture process zone

For any given aggregate size and micro silica addition level, this relation can be used to predict the fracture energy for SCC mixes. Figure 5 represents the predicted and the experimental values and shows good agreement between them. It is observed that the fracture energy increases to 42·13 N/m when the size of aggregates is varied from 6 to 12·5 mm at a micro silica addition level of 10%. When the size of coarse aggregate increases the fracture path becomes more torturous due to aggregate interlocking and bridging. Hence, higher energy is needed and also more ITZ is found in the mix having a large volume of coarse aggregates, which leads to debonding in aggregates (Beygi *et al.*, 2014a).

Considering the effect of aggregate size and micro silica addition levels a relation for the length of the fracture process zone has been developed and presented as

9. $$\text{Length} = 165{\cdot}30339 - 14{\cdot}14669 \times \text{ms} - 44{\cdot}15174 \times d_{\max} + 3{\cdot}20756 \times \text{ms} \times d_{\max} + 3{\cdot}16211 \times d_{\max}^2$$

where $d_{\max}$ is the maximum aggregate size in mm and ms is the micro silica addition level in %.

For any given aggregate sizes and micro silica addition level, this relation can be used to forecast C_f for the SCC mixes. From Figure 6 it is observed that the predicted values based on Equation 9 and the experimental values show a good agreement. The parameter C_f is in relation to the brittleness of concrete and with a decrease in the value of C_f, the brittleness increases and vice versa. Here, a maximum of 69·86 mm is obtained for the aggregate size of 12·5 mm at 5% micro silica addition level.

5. Conclusion

This study reports the effect of the size of coarse aggregate and micro silica on the fracture behaviour of SCC. Tests on notched beam specimens with varying sizes have been carried out and results are examined. The results showed that the fracture energy G_f is greatly affected by the size of coarse aggregate and tends to increase with the increase in sizes of the coarse aggregates. When the coarse aggregate size increases, the material brittleness index in terms of the effective length of process zone, C_f, also increases. Thus, concrete can be made more ductile with coarser aggregate. The experimental results agree with the previously reported results of an increase in fracture energy with an increase in the size of the coarse aggregates. Fracture energy is found to be at a maximum for 10% micro silica addition level, and for 15% addition level it tends to decrease. Also, fracture toughness is found to be a maximum for 12·5 mm aggregate size at 10% micro silica addition level. Reduction in the coarse aggregate size and an increase in micro silica addition level make concrete brittle. The decrease in fracture energy at 15% addition level is due to the increase in brittleness of the concrete. Relations between various fracture parameters and variables developed using the statistical approach and the experimental and predicted values are found to conform with each other.

Fracture parameters obtained for each SCC mix may be conveniently used to forecast failure loads of any SCC structures. It is also observed that the experimental results and predicted values with the size-effect law agree with each other. Increase in size of aggregates in SCC mixes indicated more ductile characteristics vis-à-vis smaller aggregate sizes. Frictional forces, aggregate interlocking and aggregate bridging in the fracture process zone are the major reasons for the improvement in ductility.

REFERENCES

Bazant ZP and Oh BH (1983) Crack band theory for fracture of concrete. *Materials and Structures* **16(3)**: 155–177.

Bazant ZP and Planas J (1997) *Fracture and Size Effect in Concrete and Other Quasi-Brittle Materials*. CRC Press, Boca Raton, FL, USA.

Beygi MHA, Kazemi MT, Nikbin IM *et al.* (2014a) The influence of coarse aggregate size and volume on the fracture behaviour and brittleness of self-compacting concrete. *Cement and Concrete Research* **66(12)**: 75–90.

Beygi MHA, Kazemi MT, Amiri JV *et al.* (2014b) Evaluation of the effect of maximum aggregate size on the fracture behaviour of SCC. *Cement and Concrete Research* **55**: 202–211.

Box GEP, Stuart Hunter J and Hunter WG (2005) *Statistics for Experimenters: Design, Innovation, and Discovery*, 2nd edn. Wiley, Hoboken, NJ, USA.

Craeye B, Schutter GDE, Desmet B *et al.* (2010) Effect of mineral filler type on autogenous shrinkage of self-compacting concrete. *Cement Concrete Research* **40(6)**: 908–913.

EFNARC (European Federation of National Associations Representing producers and applicators of specialist building products for Concrete) (2002) *Specification & Guidelines for Self-Compacting Concrete*, English edn. European Federation for Specialist Construction Chemicals and Concrete Systems, Norfolk, UK.

Ghaemmaghami A and Ghaemian M (2006) Large-scale testing on specific fracture energy determination of dam concrete. *International Journal of Fracture* **141(1–2)**: 247–254.

Glucklich J (1963) Fracture of plain concrete. *ASCE Journal of Engineering Mechanics Division Proceedings* **89(6)**: 127–138.

Hillerborg A, Modéer M and Petersson PE (1976) Analysis of crack formation and crack growth in concrete by means of fracture mechanics and finite element. *Cement and Concrete Research* **6(6)**: 773–781.

Jenq YS and Shah SPA (1985) Fracture toughness criterion for concrete. *Engineering Fracture Mechanics* **21(5)**: 1055–1069.

Kwon SH, Zhao Z and Shah SP (2008) Effect of specimen size on fracture energy and softening curve of concrete: part I. Experiments and fracture energy. *Cement and Concrete Research* **38(8–9)**: 1049–1060.

Moseley MD, Ojdrovic RP and Petroski HJ (1987) Influence of aggregate size on fracture toughness of concrete. *Theoretical and Applied Fracture Mechanics* **7(3)**: 207–210.

Mrudul PM, Upender T, Balachandran M and Mini KM (2017) Study on silica infused recycled aggregate concrete using the design of experiments. *International Journal of Engineering Sciences & Emerging Technologies* **12(4)**: 958–971.

Nikbin IM, Beygi MHA, Kazemi MT *et al.* (2014) Influence of mineral powder content on the fracture behaviour of SCC. *Cement and Concrete Research* **61**: 64–85.

Rilem TCS (1985) Rilem FMC-50: determination of the fracture energy of mortar and concrete by means of three-point bend tests on notched beams. *Materials and Structures* **18(4)**: 287–290.

Rilem TCS (1990) Rilem FMT-89: size-effect method for determining fracture energy and process zone size of concrete. *Materials and Structures* **23(6)**: 461–465.

Trunk B and Wittmann FH (1998) Influence of element size on fracture mechanics parameters of concrete. *Dam Engineering* **9(1)**: 3–23.

Yang C, Chong W, Tao Y *et al.* (2009) Analysis on ITZ structure of self-compacting concrete. *Proceedings of 2nd International Symposium on Design, Performance and Use of Self-Compacting Concrete SCC, Beijing, China* (Shi C, Yu Z, Khayat KH and Yan P (eds)). Rilem, Paris, France, pp. 426–434.